Frequency-specific and spatiotemporal dynamics of β-γ phase-amplitude coupling in Parkinson's disease

Philipp A. Loehrer,[1,2] Sahar Yassine,[1] Immo Weber,[2] Valentin Sanner,[3] Shenghong He,[1] Alek Pogosyan,[1] Lijiao Chen,[2] Laura Witt,[2] Gereon Rudolf Fink,[3,4] David J. Pedrosa,[2,5] Lars Timmermann[2,5] and Huiling Tan[1]

Abstract

Cross-frequency coupling (CFC) has been proposed to facilitate neural information transfer across spatial and temporal scales. Phase-amplitude coupling (PAC), a type of CFC in which the amplitude of a faster brain oscillation is coupled to the phase of a slower brain oscillation, is implicated in various higher-order cognitive functions and was shown to be pathologically altered in neurological and psychiatric disease. In Parkinson's disease (PD), the coupling between gamma amplitude (50-150 Hz) and beta phase (13-35 Hz) is exaggerated. Enhanced β-γ PAC was found in the subthalamic nucleus and various cortical sources and shown to be responsive to dopaminergic therapy and deep brain stimulation (DBS). Therefore, exaggerated β-γ PAC has been proposed to be a disease marker and a potential target for brain circuit interventions. Despite these promising findings, a significant knowledge gap remains, as the spatial and frequency-specific dynamics of β-γ PAC and its association with motor symptoms and therapy remain elusive.

To address this knowledge gap, we employed high-density electroencephalography (EEG) with source localisation techniques for patients with PD at rest.

We highlight three key findings: (1) a frequency-specific increase in high β (23-35 Hz)-γ PAC within and between sources of the cortical motor network, (2) a link between elevated high β-γ PAC and bradykinesia and rigidity when OFF medication, but not tremor, and (3) a medication-induced reduction in high β-γ PAC in the supplementary motor area correlating with clinical improvement.

Altogether, this study provides novel insights into the pathophysiology of PD as an oscillopathy and identifies high β-γ PAC as a potential marker of Parkinsonian symptoms and treatment effects.

This has important implications for invasive as well as non-invasive therapeutic strategies as high β-γ PAC targeting might hold greater promise than targeting β-γ PAC per se.

Author affiliations:

1 MRC Brain Network Dynamics Unit, Nuffield Department of Clinical Neurosciences, University of Oxford, Oxford, OX1 2JD, UK

2 Department of Neurology, Philipps-University Marburg, 35037 Marburg, Germany

3 Department of Neurology, University Hospital Cologne, 50937 Cologne, Germany

4 Cognitive Neuroscience, Institute of Neuroscience and Medicine (INM-3), Research Center Jülich, 52428 Jülich, Germany

5 Center for Mind, Brain and Behavior (CMBB), 35032 Marburg, Germany

Correspondence to: Philipp A. Loehrer

Department of Neurology

Philipps-University Marburg

Baldinger Str.

35037, Marburg, Germany

Email: loehrer@staff.uni-marburg.de

Correspondence may also be addressed to: Huiling Tan

MRC Brain Network Dynamics

Nuffield Department of Clinical Neurosciences

University of Oxford

Oxford OX1 2JD, UK

E-mail: huiling.tan@ndcn.ox.ac.uk

Running title: Characterizing cortical β-γ PAC in PD

Keywords: phase-amplitude coupling; electroencephalography; hyperdirect pathway; Parkinson's disease; β-γ PAC; θ-γ PAC

Introduction

Neural oscillations reflect the synchronised activity of neural ensembles and facilitate information processing and transfer within and between distant regions of the human brain.[1,2] In this context, cross-frequency coupling (CFC), i.e. the interaction between oscillations at different frequencies, is an important mechanism underlying information processing as larger neural populations typically oscillate at lower frequencies, while smaller ensembles are active at higher rhythms.[3,4] In particular, Phase-Amplitude Coupling (PAC), a type of CFC where the amplitude of a high-frequency oscillation is coupled to a specific phase of a low-frequency rhythm,[5] plays a significant role in various higher cognitive functions. Most notably, coupling between theta phase (4-8 Hz) to gamma amplitude (30-100 Hz) in the hippocampus has been implicated in memory and learning.[6-10] Furthermore, PAC is modulated in various activities, including visual[11] and auditory processing,[12] movement and speech,[13] as well as complex cognitive functions.[14] Additionally, changes in PAC patterns have been linked to neuropsychiatric disorders, including Parkinson's disease (PD), Alzheimer's disease, schizophrenia, and obsessive compulsive disorder.[15]

In PD, exaggerated coupling between beta phase (13-35 Hz) and gamma amplitude (50-150 Hz) has been detected in cortical and subcortical structures. In this regard, the subdivision of the beta frequency band into low-beta (13-22 Hz) and high-beta (23-35 Hz) is essential for PD pathophysiology, as these sub-bands reflect distinct neurophysiological mechanisms with different clinical implications.[16] Evidence suggests that low-beta activity in the STN is more consistently associated with overall motor symptom severity, while high-beta measures have been related to motor improvement with therapy.[16-18] In the context of PAC, emerging evidence also suggest a functional subdivision within the beta band.[16,19] Here, low β-γ PAC in the STN was associated with motor symptom severity[16] while dopaminergic medication was found to reduce high β-γ PAC in the STN when comparing the OFF and ON medication states.[19] Despite this functional segregation, most investigations of β-γ PAC have analysed beta as a unified frequency band (13-35 Hz). Nonetheless, these studies revealed important patterns across brain regions. In particular, β-γ PAC was elevated in the subthalamic nucleus (STN) and positively associated with symptom severity of bradykinesia and rigidity.[16] On the cortical level, exaggerated β-γ PAC was found in

various cortical areas,[20] including sensorimotor cortex and shown to be reduced by DBS.[21,22] Furthermore, elevated β-γ PAC was detected on the scalp level in C3/C4 using EEG, associated with bradykinesia, and shown to be amenable to dopaminergic therapy.[23,24] Given the associations between elevated PAC and symptom severity and the observed restoration to healthy levels with therapy, PAC is a promising marker for the disease and a potential target for neuromodulation therapies.[25] In contrast, cortical beta power does not consistently differentiate between medication states. Previous studies employing EEG, magnetoencephalography, or electrocorticography have reported inconsistent alterations of cortical beta power with medication,[21,23,26,27] limiting its utility for treatment monitoring and highlighting the need for alternative oscillatory markers. Despite the promising findings with PAC, a critical knowledge gap remains, as the spatial and frequency-specific dynamics of β-γ PAC on the cortical level, and its association with motor symptoms and therapy, remain elusive. To address this knowledge gap, we combined high-density electroencephalography (EEG) with source localisation techniques to characterise the spatial and frequency-specific patterns of exaggerated β-γ-PAC in PD. Using this approach, we provide evidence for a frequency-specific elevation of high β-band (23-35 Hz) to broadband-γ PAC within and between sources of the human motor network. This elevated high β to broadband-γ PAC is associated with bradykinesia and rigidity, and restoring healthy levels in the supplementary motor area (SMA) is associated with clinical improvement. Altogether, this study provides novel insights into the pathophysiology of PD as an oscillopathy and identifies high β-γ PAC as a potential marker of Parkinsonian symptoms and treatment effects.

Materials and methods

Ethical Approval

The study was approved by the local ethics committee (study number: 14-130) and carried out following the Declaration of Helsinki.

Participants

Seventeen patients with PD and fifteen healthy control subjects (HC) matched concerning age, sex, and cognitive function participated in this study upon written informed consent. Clinical

diagnosis of PD was established according to recent diagnostic criteria,[28] and motor function was assessed before and during the experiment using the Unified Parkinson's Disease Rating scale part III (UPDRS-III). All participants were right-handed, according to the Edinburgh Handedness Inventory. There was no indication of depressive symptoms or dementia according to Beck's Depression Inventory-II and Mini-Mental State Examination. Exclusion criteria during participant recruitment comprised pathological MRI findings, concomitant neurological or psychiatric disease, or impaired visual or auditory function. Two healthy controls and one patient had to be excluded due to severe artefacts interfering with the EEG recording. One patient had to be excluded as he discontinued MRI acquisition and subsequent EEG recordings due to claustrophobia, whereby no participant had to be excluded due to pathological MRI findings. Following preprocessing, the datasets of 15 patients (mean age±SD: 68.2±8.2 years; 2 female) and 13 healthy controls (mean age±SD: 64.4±6.5 years; 1 female) were included for further analysis (for demographics see Table 1). Patients and healthy controls were well matched for age and gender ($p = .21$).

Data Acquisition

EEG-data were acquired using a 128-channel system with active electrodes (Brain Products GmbH, Gilching, Germany) and a reference channel on FCz, in an acoustically and electrically shielded room. Individual positions of electrodes and fiducial points were acquired using a 3D ultrasound digitisation system (Zebris Medical GmbH, Isny, Germany). After assuring that electrode impedances were below 10 kΩ, EEG-signals were recorded with Brainvision recorder (Brain Products GmbH, Gilching, Germany). Here, signals were amplified, band-pass filtered from 0.1 to 1000 Hz, and digitised at a sampling rate of 5000 Hz. The experimental paradigm consisted of multiple trials with 15 seconds of continuous resting state and various movement tasks including tapping with an external stimulus and tapping without an external stimulus, each followed by a 5-second pause. Only data from the rest condition was analysed for this report, whereby data from the movement tasks have not been published elsewhere. Given the randomised order and the pause duration, it is unlikely that movement preparation influenced the resting-state data. During the resting state recordings, participants were instructed to relax and focus on a cross presented on a screen before them. EEG of patients with PD was recorded in medication OFF, after 12 hours of withdrawal of antiparkinsonian medication, and in medication ON, following the administration

of 200 mg levodopa. In all patients, an experienced movement disorders specialist (PAL) assessed the UPDRS-III in the OFF and ON state.

Before EEG recordings, individual T1-weighted MRI of the head were acquired on a 3-Tesla Trio scanner (Siemens, Erlangen, Germany) using a 3D Modified Driven Equilibrium Fourier Transform sequence (repetition-time = 1930 ms, echo-time = 5.8 ms, flip-angle = 18°, slice-thickness = 1 mm) for individual source reconstruction.

EEG Preprocessing

Preprocessing was performed using Fieldtrip.[29] First, data were demeaned and detrended, high-pass filtered at 1 Hz, low-pass filtered at 500 Hz, and band-stop filtered at 50 Hz and its harmonics. Then, data were downsampled to 1000 Hz and epoched into non-overlapping segments of 3000 ms, as it has been shown that PAC can be detected robustly in epochs of 2500 ms and longer at different levels of noise and coupling strength.[30,31] Subsequently, an independent component analysis was used to remove components containing eye movements, channel noise, muscle-, and electrocardiogram-artefacts. Segments were visually inspected, and channels and segments with poor data quality were excluded. Excluded channels were interpolated (20.5 +/- 1.9 channels for each patient and 19.4 +/- 2.9 channels for each healthy control), and a final visual inspection of the data was performed. If artefacts affected over 50% of the data segments, the entire dataset was excluded from subsequent analysis. As a result of this process, two healthy controls and one patient were excluded from the study. Following the removal of all artefacts, there were no significant differences in data volume, i.e. segments, between patients and controls (28.9 +/- 2.8 segments for each patient and 32.9 +/- 7.2 segments for each healthy control, $p = 0.78$). In a last step, data were re-referenced to the average reference of all electrodes.

EEG-MRI Coregistration and 3D Cortical Mesh Construction

To reconstruct the dynamics of the brain at the cortical-source level, the inverse problem was solved based on the artefact-free EEG data and patients structural MRI employing source localisation techniques, i.e. the combination of individual structural MRI, mapping of a multi-modal cortex parcellation, and beamforming. Here, functions from Freesurfer (http://surfer.nmr.mgh.harvard.edu/, version: 7.4.1), Brainstorm (version: 10-Oct-2023), and custom MATLAB (R2020b) scripts were employed. The procedure is outlined in **Figure 1** and included segmentation of individual MRIs and parcellation using the Human Connectome Project

(HCP) atlas.[32] Here, we retained a fine resolution for motor regions, which resulted in 26 regions per hemisphere. EEG data were co-registered with the segmented MRI, and a realistic head model was generated employing the OpenMEEG boundary element method.[33] Further methodological details are provided in the Supplementary material.

Region of interest-based Source Reconstruction

Source analysis was performed utilising a linearly constrained minimum variance beamformer (LCMV).[34] This technique applies a spatial filter to the EEG data at each vertex of the 3D cortical mesh, aiming to maximise the signal from that particular location while suppressing signals from other areas.[31] The spatial filter was constructed by combining the covariance matrix obtained from the sensor data with the leadfield information obtained from the head model. To extract a single source signal for each region of interest in the cortical motor network (dorsolateral prefrontal cortex (DLPFC), lateral premotor cortex (lPM), primary motor cortex (M1), supplementary motor area (SMA)),[35,36] we constructed a single spatial filter for each ROI by calculating the mean of the concatenated filters from all vertices identified to lie within a ROI. Sensor-level data was then multiplied with this spatial filter to extract the source time series for each ROI. In a supplementary analysis, we extracted source time series for each ROI in the cortical motor network employing minimum norm imaging.[37] To display whole brain source distributions of PAC, we extracted source time series data for each region defined by our approach and calculated PAC as outlined below.

Phase-Amplitude Coupling Analysis

Source time series were examined for β-γ phase-amplitude coupling employing the Kullback-Leibler-based modulation index.[38] As a first step, trials were zero-padded with segments of 750 ms, which were discarded after filtering, as spurious PAC can occur through filtering sharp edge artefacts.[39] Subsequently, low-frequency phase and high-frequency amplitude were extracted from each trial's source time-series, employing a 2-way finite impulse response filter (eegfilt.m with fir1 parameters). Here, source time series were filtered across the 4 to 50 Hz range using a sliding window with a step size of 2 Hz and a bandwidth of 2 Hz to extract phase. Similarly, source time series were filtered across the 4 to 200 Hz range using a sliding window with a step size of 4 Hz to extract amplitude, as described previously.[21,23] As the bandwidth for filtering the amplitude-providing time series should depend on the frequency of the phase-providing frequency,[31] the

bandwidth was chosen to be wide enough to capture the centre frequency ± the modulating low-frequency phase. Subsequently, instantaneous phase and amplitude were extracted from the filtered signals using a Hilbert transform.

To calculate the modulation index, phases from -180° to 180° were first binned into 18 bins of 20° each.[38] Subsequently, the mean amplitude of the amplitude-providing frequency in each phase bin of the phase-providing frequency was calculated and normalised by the sum of the mean amplitudes for all bins. This created an amplitude-phase distribution similar to a probability distribution, which was then quantified using Shannon entropy. As Shannon entropy represents a variable's inherent amount of information, it is maximal, if – in this context – the amplitude in each phase bin is equal.[30] This would represent a uniform distribution and correspond to the absence of phase-amplitude coupling. To measure the disparity between the calculated distribution and a uniform distribution, the Kullback-Leibler distance is calculated to derive the modulation index (MI), which is defined as PAC. To quantify the meaningfulness of the derived MI-values, remove forms of spurious coupling, and make MI-values amenable to statistical evaluation, we performed nonparametric permutation testing.[23,30] Here, we defined zPAC as z-scored MI values by comparing the observed MI-value to a surrogate distribution of MI-values based on shuffled data. This surrogate distribution was generated by temporally shifting the phase time series compared to the amplitude time series. The phase time series was circularly shifted by cutting it at a randomly selected point within its length, effectively introducing a random temporal offset. Phase-amplitude coupling was then calculated, and this procedure was repeated 200 times. Thus, a zPAC value of 0 indicates a PAC level similar to that of randomly shuffled data, while a zPAC value greater than 1.64 suggests significant coupling, indicating less than a 5% probability of occurring by chance.

To ensure that residual line noise artefacts did not affect PAC calculation, we recalculated β-γ PAC with frequency ranges excluding 50 Hz and its harmonics (Supplementary material). Furthermore, we performed a sensitivity analysis comparing β-γ PAC in segments from the first and second halves of each 15-second resting period block to verify that movement preparation did not influence PAC values in the latter segments (Supplementary material).

Power spectral density

To exclude the possibility that differences in spectral power in either β- or γ-band drive enhanced PAC, we calculated the power spectral density (PSD) of the different re-constructed source regions using the Welch method (Supplementary material).

Non-Sinusoidal Oscillations

Another significant challenge encountered in the analysis of PAC involves the presence of non-sinusoidal oscillations, which can lead to spurious PAC.[40-42] The characteristics of an oscillation were assessed by computing sharpness and steepness ratios for the time series data of each ROI in the 13 to 35 Hz range (Supplementary material).

Simulated PAC Analysis

The reliability of our PAC algorithm was tested on 3 seconds of simulated data containing predetermined β-γ PAC (Supplementary material).

Statistical Analysis

Group statistics were performed to compare β-γ PAC among patients in the medication ON and OFF state, and between patients and healthy controls. A repeated measures ANOVA was employed to analyse PAC differences within patients, with the repeated measures factors 'source' (e.g., cortical regions of interest), 'frequency' (e.g., low (13-22 Hz) and high (23-35 Hz) β-γ PAC values), the independent variable 'medication state' (ON or OFF), and the covariate 'hemisphere' (left or right), using Greenhouse-Geisser correction for non-sphericity when appropriate. A mixed design ANOVA was performed for comparisons between patients and HC, with the within-subjects factors 'source' and 'frequency', the between-subjects factor 'group' (PD or HC), and the covariate 'hemisphere' (left or right). All statistical analyses were conducted to test for main effects and interactions between factors. Post-hoc analyses were performed where appropriate to identify significant pairwise comparisons. For statistical comparison, a zPAC value was derived for each subject by averaging the comodulograms of the regions of interest. To delineate differences in high and low β-γ PAC, we averaged MI values over the low beta-band (13-22 Hz) as well as the high-beta band (23-35 Hz) for the phase frequency and the broadband gamma range (50-150 Hz) for the amplitude-frequency. These frequency ranges were chosen based on prior research,[20,23,43] whereby power analyses and analyses of sinusoidal oscillations focused on the

same frequency ranges. In a supplementary analysis, we averaged MI values over the theta-band (4-8 Hz) as well as the alpha band (8-12 Hz) for the phase frequency and the broadband gamma range (50-150 Hz) for the amplitude frequency. Averaged MI values were squareroot-transformed to fulfil assumptions of ANOVA testing. Spearman correlations were used to investigate the relationship between β-γ PAC, clinical features, and treatment response, corrected for multiple comparisons using the Benjamini-Hochberg method.[44] Exploratory analyses assessing θ-γ and α-γ PAC and supplementary analyses assessing data with frequency ranges excluding 50 Hz and its harmonics, sub-band differences in β PSD, as well as β-γ PAC calculated from source time series obtained via minimum norm imaging were performed employing the same statistical approach as described above.

Results

Phase-amplitude coupling within sources of the human motor network is enhanced in Parkinson's disease

We assessed the effects of participant group (PD OFF vs. HC), frequency for phase (low β vs. high β), and each considered source on β-γ PAC using a three-way mixed-design ANOVA. This analysis demonstrated significant main effects of 'group' ($F(1,26) = 5.76$, $p = .02$, $\eta_p^2 = .098$, **Supplementary Figure 1**) and 'frequency' ($F(1,27) = 5.39$, $p = .024$, $\eta_p^2 = .092$), but not 'source' ($F(3,81) = .95$, $p = .41$, $\eta_p^2 = .018$). Here, β-γ PAC was higher in patients OFF medication than HC. The effect, however, was present for high β-γ PAC (high β: 23-35 Hz; frequency x group interaction: $F(1,26) = 6.41$, $p = .014$, $\eta_p^2 = .11$), but not for low β-γ PAC (low β: 13-22 Hz). Post hoc t-tests for the different ROIs demonstrated that high β-γ PAC was increased in patients in M1 ($t(26) = -2.28$, $p = .014$, Cohen's $d = .58$) and lPM ($t(26) = -2.96$, $p = .003$, Cohen's $d = .75$, **Figure 2**). The mixed design ANOVA comparing patients ON medication and HC revealed no significant difference in overall β-γ PAC between the two groups ($F(1,26) = 0.05$, $p = .944$, $\eta_p^2 = <.001$) and between sources ($F(3,81) = 2.49$, $p = .079$, $\eta_p^2 = .045$). However, a significant main effect of **'frequency'** ($F(1,27) = 9.78$, $p = .003$, $\eta_p^2 = .156$) indicated differences in β-γ PAC across frequency bands. Additionally, no interaction between frequency-band and group existed ($F(1,26) = 0.02$, $p = .961$, $\eta_p^2 = <.001$).

We assessed the effects of medication status (PD OFF vs. PD ON), frequency for phase (low β vs. high β) and each considered source on β-γ PAC using a three-way repeated measures ANOVA. The analysis demonstrated significant main effects of 'medication' ($F(1,26) = 6.37$, $p = .014$, $\eta_p^2 = .101$) and 'frequency' ($F(1,27) = 5.66$, $p = .021$, $\eta_p^2 = .09$), whereas no significant main effect of 'source' was observed ($F(3,81) = .48$, $p = .683$, $\eta_p^2 = .008$). Here, patients OFF medication had higher overall β-γ PAC values than ON medication. This effect was present for high β-γ PAC only (frequency x medication interaction: $F(1,26) = 7.98$, $p = .007$, $\eta_p^2 = .123$). Post hoc paired t-tests for the different ROIs demonstrated that high β-γ PAC was increased in patients OFF medication in M1 ($t(14) = -1.81$, $p = .04$, Cohen's $d = .47$), lPM ($t(14) = -2.39$, $p = .011$, Cohen's $d = .6$), and SMA ($t(14) = -2.73$, $p = .005$, Cohen's $d = .66$), whereby a trend towards significance was observed for DLPFC ($t(14) = -1.68$, $p = .052$, Cohen's $d = .36$; **Figure 3**). The supplementary analyses employing source time series data obtained via minimum norm imaging as well as data with frequency ranges excluding 50 Hz and its harmonics revealed consistent results (Supplementary material).

In the OFF medication state, correlation analysis revealed a significant relationship between high β-γ PAC and UPDRS-OFF values in M1 ($p = .04$, $rho = .535$), lPM ($p = .04$, $rho = .569$), and SMA ($p = .049$, $rho = .475$, **Supplementary Figure 2**). Furthermore, high β-γ PAC values were correlated with the bradykinesia-rigidity subscore in M1 ($p = .035$, $rho = .521$), lPM ($p = .035$, $rho = .509$), and SMA ($p = .035$, $rho = .543$, **Supplementary Figure 3**) but not with the tremor subscore (all $p > .43$). There were no correlations between high β-γ PAC and UPDRS-ON values (all $p > .066$).

As prior studies have demonstrated an association between medication effects on electrophysiological markers and clinical subscores of the predominantly affected side,[24] we sought to evaluate the impact of medication on high β-γ PAC and clinical parameters. Specifically, we correlated the percentage change in high β-γ PAC of the ROIs contralateral to the primarily affected side with the percentage change in the UPDRS-III score and its subscores of the primarily affected side. Here, medication-induced change in high β-γ PAC of the SMA correlated with overall symptom improvement ($p = .004$, $rho = .731$) as well as improvement of bradykinesia and rigidity ($p = .002$, $rho = .758$) but not with tremor improvement ($p = .11$, $rho = .569$, **Figure 4**). This effect remained significant even after excluding outliers (UPDRS-III: $p = .041$, $rho = .683$;

bradykinesia-rigidity subscore: p = .046, rho = .691, **Supplementary Figure 4**). All p-values are corrected for multiple comparisons using the Benjamini-Hochberg method.

Phase-amplitude coupling between sources of the human motor network is enhanced in Parkinson's disease

We assessed the effects of participant group, interconnected sources, and frequency for phase (high β vs. low β) on inter-source β-γ PAC using three-way mixed design and repeated measures ANOVA. For conciseness, only significant group effects and post hoc tests are reported here; full results are in the Supplementary material.

Inter-source β-γ PAC was significantly higher in patients OFF medication compared to HC ($F(1,26) = 4.92$, $p = .031$, $\eta_p^2 = .085$, **Supplementary Figure 5**). This effect, however, was present for high β-γ PAC (frequency x group interaction: $F(1,26) = 5.08$, $p = .028$, $\eta_p^2 = .087$) but not low β-γ PAC. Post hoc testing revealed increased high β-γ PAC between several sources of the cortical motor network in patients, with significant connections summarized in Table 2. No differences between patients ON medication and HC were observed ($F(1,52) = .12$, $p = .727$, $\eta_p^2 = .002$).

Within patients, inter-source β-γ PAC was significantly higher OFF versus ON medication ($F(1,26) = 4.87$, $p = .031$, $\eta_p^2 = .079$), this effect was present for high β-γ PAC (frequency x group interaction: $F(1,52) = 6.16$, $p = .016$, $\eta_p^2 = .098$) but not low β-γ PAC. Post hoc testing demonstrated increased high β-γ PAC OFF medication between multiple sources of the cortical motor network, with significant results summarized in Table 2. No correlations between interregional β-γ PAC and clinical scores were present after correcting for multiple comparisons.

Exploratory analyses of α-γ and θ-γ phase-amplitude coupling within sources of the human motor network

Exploratory analyses of α-γ and θ-γ PAC were performed, although mean zPAC values remained below the significance threshold of 1.64, to characterise the frequency profile relative to β-γ PAC. For conciseness, only significant group effects and post hoc tests are reported here; full results are in the Supplementary material. These findings should be interpreted with caution given the overall low coupling strength.

The omnibus ANOVA across all frequency bands (θ-γ, α-γ, low/high β-γ) confirmed significant group effects (PD OFF vs HC: $F(1,26) = 9.01$, $p = .004$, $\eta p^2 = .145$) with a frequency × group

interaction ($F(3,78) = 3.68$, $p = .013$, $\eta p^2 = .065$). Here, high β-γ PAC exceeded θ-γ/α-γ PAC across all ROI ($p \leq .001$). Similarly, for PD OFF vs ON, significant medication ($F(1,26) = 11.44$, $p = .001$, $\eta p^2 = .167$) and interaction effects ($F(3,78) = 3.75$, $p = .012$, $\eta p^2 = .062$) were confirmed, with high β-γ PAC exceeding θ-γ/α-γ PAC across all ROI ($p \leq .001$).

The α-γ PAC was significantly higher in patients OFF medication compared to HC ($F(1,26) = 5.56$, $p = .022$, $\eta_p^2 = .095$), with strongest effects in lPM ($p = .012$). No differences between patients ON medication and HC were observed ($F(1,26) = 2.74$, $p = .1$, $\eta_p^2 = .049$). Within patients, α-γ PAC was significantly higher OFF versus ON medication ($F(1,26) = 15.71$, $p < .001$, $\eta_p^2 = .216$), with significant increases in lPM ($p = .002$), M1 ($p = .005$), and SMA ($p < .001$).

θ-γ PAC was significantly higher in patients OFF medication compared to HC ($F(1,26) = 10.53$, $p = .002$, $\eta_p^2 = .166$), with significant differences in M1 ($p = .001$), lPM ($p = .017$), and SMA ($p = .012$). No differences between patients ON medication and HC were observed ($F(1,26) = .003$, $p = .95$, $\eta_p^2 = < .001$). Within patients, θ-γ PAC was significantly higher OFF versus ON medication ($F(1,26) = 10.68$, $p = .002$, $\eta_p^2 = .158$), with significant increases in lPM ($p = .019$), M1 ($p = .038$), and SMA ($p = .005$). Given prior links between tremor and low-frequency oscillations[45,46] we explored the relationship between PAC and clinical parameters. Medication-induced reductions in θ-γ PAC within lPM contralateral to the primarily affected side correlated with improvements in both tremor ($p = .049$, rho = .694) and bradykinesia-rigidity ($p = .039$, rho = .685). P-values are corrected for multiple comparisons using the Benjamini-Hochberg method.

Visualisation of source distributions of PAC clearly demonstrate the influence dopamine exerts on the cortical level (see **Figure 5, Supplementary Figure 6, and Supplementary Figure 7**). It also highlights that these effects are frequency specific within the investigated ROI (DLPFC, lPM, M1, SMA), with pronounced differences observed particularly in the high β-γ PAC range (**see Supplementary Figure 8**).

Power spectral density

No differences in β- or γ-band in patients with PD ON and OFF medication compared to HC were detected (all $p > .09$; **Supplementary Figure 9** and **Supplementary Figure 10**). Analyses assessing sub-band differences in β PSD and the association between β PSD and clinical scores are reported in the Supplementary material.

Non-sinusoidal Oscillations

No differences in the β-band between groups were detected in sharpness and steepness ratios (all $p > .57$), suggesting that our results are unlikely to be undermined by differences in waveform shapes (**Supplementary Figure 11** and **Supplementary Figure 12**).

Simulated phase-amplitude coupling

Using our PAC algorithm, we were able to successfully detect β-γ PAC in simulated data segments with known β-γ PAC, supporting the validity of our algorithm. (**Supplementary Figure 13**).

Discussion

In the present study, we used high-density EEG combined with source localisation techniques to characterise the spatial and frequency-specific patterns of exaggerated β-γ phase-amplitude coupling in Parkinson's disease. There are three key findings. First, we demonstrate a frequency-specific elevation of β-γ PAC within and between sources of the human motor network with the phase of high β-band but not low β-band oscillations modulating the power of γ-band activities. Second, we identify an association between elevated high β-γ PAC with bradykinesia and rigidity within distinct sources of the motor network when patients were OFF medication. Tremor scores, however, were not associated with elevated β-γ PAC. Finally, medication-induced high β-γ PAC reduction within the SMA was associated with clinical improvement. Altogether, this study identifies high β-γ PAC as a potential cortical marker of Parkinsonian symptoms and treatment effects with implications for targeted strategies.

High β-γ PAC is elevated in the cortical motor network

In PD, elevated β-γ phase-amplitude coupling has been detected in cortical and subcortical structures using invasive and non-invasive techniques.[47] In particular, elevated β-γ PAC was observed within the STN and associated with symptom severity of bradykinesia and rigidity.[16] On the cortical level, β-γ PAC across the beta frequency range (13-30 Hz) was elevated over the sensorimotor cortex as assessed by ECoG as well as EEG and was responsive to dopamine replacement therapy and DBS.[21-23] In line with previous findings, we identified elevated β-γ PAC within areas of the cortical motor system. We extend these findings by identifying a frequency-specific elevation of PAC, including high-β to broadband-γ PAC. Low-β-γ PAC, however, was

not elevated in patients with PD. The β-band has been subdivided into low- (13-22 Hz) and high-β (23-35 Hz) to differentiate the roles of distinct frequencies in PD symptoms and to provide a more nuanced understanding of neural oscillations in normal and pathological states. In particular, Binns and colleagues[48] show that high beta power within the primary motor cortex can be associated with bradykinesia and decreased after dopaminergic treatment. At the subcortical level, STN low-beta oscillations have been associated with UPDRS-III total scores, while high-beta oscillations have been related to UPDRS-III response to levodopa and DBS therapy.[17] Moreover, recent studies employing invasive recordings suggest an association between cortico-subcortical coupling in beta sub-bands and anatomical pathways.[48-50] While M1-STN coupling in the low-beta band is supposed to be a surrogate of indirect pathway activity, M1-STN high-beta coupling might be a surrogate of hyperdirect pathway activity, which has been hypothesised to mediate the therapeutic effects of DBS and dopaminergic therapy.[48] Using invasive recordings, such as electrocorticography, bears the advantage of high spatial resolution and low signal-to-noise ratio. Spatial coverage, however, is limited due to the size of the electrode strip that can be placed through a burr hole, and the widespread employment in clinical practice is limited due to its invasive nature.[20] Using source localisation techniques, we overcame the limitations of spatial coverage and the invasive nature of ECoG recordings. Our results show that elevated high β-γ PAC is present not only in somatosensory areas but extends to additional areas of the cortical motor system, including lPM. This is in line with the results by Gong and colleagues,[20] who showed that β-γ PAC was elevated in cortical sources, including premotor cortex (PMC) and BA3 and consistent with findings demonstrating the involvement of PMC in PD.[51] While exploratory analyses also revealed group differences in α-γ and θ-γ PAC, the absolute zPAC values were below the significance threshold and markedly higher for high β-γ PAC, surpassing the significance threshold and α-γ and θ-γ PAC across all ROI and contrasts (see Figure 5). Importantly, the omnibus analysis including all frequency bands confirmed that this increase was most pronounced for high β-γ PAC. Furthermore, high β-γ PAC showed associations with clinical outcomes. However, it is important to note that β-γ PAC is not a disease-specific phenomenon but more likely a fundamental physiological mechanism[52] that becomes exaggerated in PD. Healthy controls in our study showed significant high β-γ PAC, consistent with findings from people without movement disorders in prior studies.[21,52] Therefore, the critical distinction in PD is pathological exaggeration rather than de novo emergence. Altogether, our findings suggest a frequency-specific

profile and corroborate the notion that β-γ PAC is a potential marker for the Parkinsonian state but highlight the importance of subdividing the beta band to allow for more precise approaches in differentiating between healthy controls and patients with PD. Moreover, we further extend the findings by Gong and colleagues[20] by showing that β-γ PAC was elevated between sources of the cortical motor network. Functional and induced connectivity analyses showed distinct alterations in patients within the cortical motor network.[53,54] In particular, enhanced β-γ coupling between primary motor cortices was associated with poor motor performance and prefrontal to premotor coupling is pathologically altered in PD.[54] Accordingly, we found exaggerated high β-γ PAC between prefrontal and premotor areas and between prefrontal cortex and primary motor cortex in patients with PD. As effect sizes of post-hoc comparisons of high β-γ PAC between HC and patients were larger within cortical sources compared to between sources, our results suggest that high β-γ PAC within lPM and M1 may have the potential as a marker to differentiate between patients with PD and healthy controls. However, further studies with larger samples using classification algorithms would be needed to confirm this. In line with previous studies[23,55] and supported by our supplementary analyses, we found no difference in cortical beta power between healthy controls and patients with PD. In contrast, we observed that cortical high β-γ PAC was elevated in PD and correlated with clinical features. Altogether, these findings reinforce the importance of delineating the frequency-specific characteristics of β-γ PAC within the cortical motor system and shed light on the potential role of high β-γ PAC as a diagnostic marker.

Dopaminergic therapy reduces elevated high β-γ PAC in the motor network

Given the excessive increase in cortical β-γ PAC, several studies have investigated the effects of dopaminergic therapy and DBS on PAC. In particular, de Hemptinne *et al.*[22] showed that DBS reduces β-γ PAC in M1 and suggested a potential role in mediating the clinical effects of DBS. Furthermore, Miller and colleagues[24] showed an impact of levodopa on PAC at the sensor level. The present study sheds light on multiple aspects of dopaminergic influence on β-γ PAC at the cortical level, most prominently demonstrating that exaggerated high β-γ PAC is reduced in all sources of the cortical motor network by dopaminergic therapy. This corroborates the results by de Hemptinne and Miller and confirms the widespread influence dopaminergic medication exerts on the cortex. Importantly, the significant interaction between medication and frequency suggests

that levodopa exerts a frequency-specific effect at the cortical level, specifically reducing exaggerated high β-γ PAC, while low β-γ PAC is not significantly influenced. Interestingly, recent findings by Binns *et al.*[48] demonstrate that levodopa selectively reduces high beta power over the primary motor cortex in PD. While our study focuses on β-γ PAC, both results support the notion of frequency-specific effects of dopaminergic treatment on cortical activity. The role of cortical beta oscillations in differentiating between medication states remains, however, controversial, as previous studies have not shown a consistent alteration with medication.[21,23,26,27] Altogether, high β-γ PAC may serve as a sensitive marker to differentiate between medication states and might be promising for treatment surveillance. In this approach, cortical signals could be sensed using an electrocorticography array to automatically adjust stimulation timing or intensity, while stimulation is delivered via depth electrodes, ensuring spatial separation between sensing and stimulation sites.[56] The therapy could also involve pump-based drug delivery or non-invasive stimulation methods such as transcutaneous vagus nerve stimulation. This approach reduces the contamination of the feedback signal by stimulation artefacts and leverages the enhanced signal-to-noise ratio provided by cortical recordings.[56] Our results are further corroborated as we demonstrate a frequency-specific reduction of high β-γ PAC between cortical sources induced by dopaminergic therapy.

High β-γ PAC is associated with motor symptoms and clinical improvement

Further support for the importance of delineating the frequency-specific dynamics of β-γ PAC comes from our observation that symptom severity was associated with high β-γ PAC. In line with previous studies, our observed associations reinforce the role of β-γ PAC in impaired motor control and highlight its potential as a marker for disease severity.[20,24] Our findings extend prior research by demonstrating that this association is frequency-specific, as no associations were observed for low β-γ and α-γ PAC. Furthermore, we show that this frequency-specific association is present within all sources of the motor network except DLPFC. This is particularly relevant for two reasons. First, identifying the specific areas where PAC is associated with clinical symptoms could help refine diagnostic and treatment strategies as therapies targeting PAC could adapt to the spatial and frequency-specific dynamics. Regions identified to show associations between cortical signals and clinical symptoms could guide the placement of sensing devices such as electrocorticography

arrays. Therapy could then be precisely adjusted to target high β-γ PAC rather than the entire β-γ spectrum. Furthermore, non-invasive approaches like transcranial magnetic stimulation might also employ high β-γ PAC as a marker to tailor stimulation to symptom-relevant sites. Second, we did not observe any associations of β-γ PAC between sources and clinical symptoms. Therefore, assessing high β-γ PAC within sources of the motor network seems more promising to establish an objective diagnostic measure than evaluating PAC between sources. We further delineate the observed associations by showing that high β-γ PAC is associated with bradykinesia-rigidity subscores. At the same time, tremor scores were not related to β-γ PAC within and between sources of the motor network. Given prior links between tremor and low-frequency oscillations,[45,46] and as emerging literature suggests that θ-γ PAC can be modulated by dopaminergic therapy and is functionally relevant for motor performance,[57,58] we explored the relationship between θ-γ/α-γ PAC and clinical parameters. These analyses suggested that medication-induced reductions in θ-γ PAC in lPM may relate to improvements in both tremor and bradykinesia-rigidity. As these correlations were present for both tremor and bradykinesia-rigidity, they do not indicate tremor-specificity. Given that θ-γ zPAC values remained below the predefined significance threshold, these exploratory correlations should be interpreted with caution as the clinical meaningfulness of this weak coupling remains to be determined. Therefore, these findings should be considered hypothesis-generating and require replication in independent cohorts.

Finally, we demonstrate an association between therapy-induced changes in β-γ PAC and therapy-induced changes in clinical severity. Specifically, a reduction in high β-γ PAC within the SMA was linked to improvements in overall motor symptoms, with a particular impact on reducing bradykinesia and rigidity.

Several considerations have to be taken into account when interpreting the finding. First, cortical layer 5 neurons in the SMA project monosynaptically to the STN via the hyperdirect pathway.[59] Recent studies have highlighted this cortical input to the STN via the hyperdirect pathway as a central contributor to pathological synchrony within the STN and between the cortex and STN.[48-50] Furthermore, Oswal and colleagues[50] demonstrated that high beta activity in the SMA drives STN activity via the hyperdirect pathway, and this pathway has widely been considered the main target for the therapeutic effects of dopaminergic therapy and DBS. While our data are limited to cortical PAC only and do not measure STN activity or cortico-STN coupling, high β-γ PAC within the SMA may represent a cortical marker that could be explored as a target for adaptive treatment

approaches, whether invasive (such as DBS or pump-therapy) or non-invasive, enabling personalised therapy. In the context of connectomic neuromodulation, our results complement recent findings by Hollunder *et al.*[51] demonstrating that in PD, optimal therapeutic outcomes are linked to modulation of STN connections to PMC and SMA, rather than to the M1. Altogether, we suggest that high β-γ PAC within the cortical motor network can serve as a marker to differentiate patients with PD from healthy controls, might be suitable for objectively assessing disease states, and might serve as an input for adaptive treatment approaches.

Limitations

This research is not without its limitations. First, analyses were conducted on recordings while patients were at rest. Therefore, our findings do not permit a direct association between elevated β-γ PAC and the clinical phenotype. Nonetheless, the observed associations between specific PAC properties and Parkinsonian motor symptoms and between PAC change and symptom improvements suggest that exaggerated PAC likely represents a marker of the Parkinsonian state. Second, the ill-posed nature of the EEG inverse problem, which states that multiple solutions for source localisation exist, applies to our source reconstruction approach. To mitigate concerns about methodological dependency, we performed supplementary analyses replicating all major findings using minimum norm imaging. While some minor differences in statistical power were observed, results were broadly consistent, supporting the validity of our approach. Third, a significant challenge in analysing cross-frequency coupling, such as PAC, is the presence of non-sinusoidal sawtooth-like oscillations, which can produce spurious PAC.[31] The characteristics of an oscillation can be quantified by determining specific temporal features, including rise- and decay-time and the ratio between them. As we observed no differences in these measures across the three groups, our results are unlikely affected by the oscillations' non-sinusoidal properties. Fourth, patients with PD who participated in this study had the akinetic-rigid and mixed subtypes. No patients with tremor-dominant subtype were included. This restricts the generalisability of our findings across all Parkinson's disease phenotypes.

Conclusion

Our study identifies high β-γ PAC as a potential biomarker for the Parkinsonian state and therapeutic strategies. Within the cortical motor network, high β-γ PAC was found to be

elevated and subsequently attenuated by dopaminergic replacement therapy. Furthermore, high β-γ PAC was correlated with bradykinesia and rigidity, and the medication-induced reduction of high β-γ PAC in the supplementary motor area was associated with improvements in these symptoms. Altogether, these findings offer further insight into the pathophysiology of PD as an oscillopathy and provide a possible foundation for future therapeutic interventions targeting specific cortical oscillatory activity.

Data availability

The data supporting the present findings are available on request from the corresponding author (PAL). The data are not publicly available due to privacy or ethical restrictions. All tools used to analyse MRI data are based on FreeSurfer Version 7.4.1,[60] which is freely available. Tools employed to analyse EEG data are based on custom MATLAB scripts as well as Brainstorm version 20231010,[61] FieldTrip version 20211020,[29] and OpenMEEG,[33] which are available online.

Acknowledgements

The authors thank the participants for their active engagement in this study.

Funding

P.A.L. was supported by the SUCCESS-Program of the Philipps-University of Marburg, the 'Stiftung zur Förderung junger Neurowissenschaftler', and the Prof. Klaus Thiemann Foundation. S.Y. was supported by the Medical Research Council (MC_UU_0003/2, MR/V00655X/1, MR/P012272/1), the MLSTF from the University of Oxford, the NIHR Oxford BRC, and the Rosetrees Trust, UK. I.W. has nothing to disclose. V.S. was supported by the Koeln Fortune Program/ Faculty of Medicine, University of Cologne. S.H. was supported by a Non-clinical Postdoctoral Fellowship from the Guarantors of Brain and an International Exchanges Award (IES\R3\213123) from The Royal Society. A.P. was supported by the Medical Research Council (MC_UU_0003/2, MR/V00655X/1, MR/P012272/1), the MLSTF from the University of Oxford, the NIHR Oxford BRC, and the Rosetrees Trust, UK. L.C. has nothing to disclose. L.W. has nothing to disclose. G.R.F. receives grants from the Deutsche Forschungsgemeinschaft (DFG, German Research Foundation), Project-ID 431549029, SFB 1451. D.J.P. has received honoraria for speaking at symposia sponsored by Boston Scientific Corp, Medtronic, AbbVie Inc, Zambon and Esteve Pharmaceuticals GmbH. He has received honoraria as a consultant for Boston Scientific Corp and Bayer, and he has

received a grant from Boston Scientific Corp for a project entitled "Sensor-based optimisation of Deep Brain Stimulation settings in Parkinson's disease" (COMPARE-DBS). The institution of D.J.P., not D.J.P. personally, has received funding from the German Research Foundation, the German Ministry of Education and Research, the International Parkinson Foundation, the Horizon 2020 programme of the EU Commission and the Pohl Foundation in Marburg. Finally, D.J.P. has received travel grants to attend congresses from Esteve Pharmaceuticals GmbH and Boston Scientific Corp. L.T. received payments as a consultant for Medtronic Inc. and Boston Scientific and received honoraria as a speaker on symposia sponsored by Bial, Zambon Pharma, UCB Schwarz Pharma, Desitin Pharma, Medtronic, Boston Scientific, and Abbott. The institution of L.T., not L.T. personally, received funding by the German Research Foundation, the German Ministry of Education and Research, and Deutsche Parkinson Vereinigung. H.T. was supported by the Medical Research Council (MC_UU_0003/2, MR/V00655X/1, MR/P012272/1), the MLSTF from the University of Oxford, the NIHR Oxford BRC, and the Rosetrees Trust, UK.

Competing interests

The authors report no competing interests.

Supplementary material

Supplementary material is available at *Brain* online.

References

1. Singer W. Neuronal Synchrony: A Versatile Code for the Definition of Relations? *Neuron*. 1999/09/01/ 1999;24(1):49-65. doi:https://doi.org/10.1016/S0896-6273(00)80821-1

2. Siegel M, Donner TH, Engel AK. Spectral fingerprints of large-scale neuronal interactions. *Nature Reviews Neuroscience*. 2012/02/01 2012;13(2):121-134. doi:10.1038/nrn3137

3. Buzsaki G. *Rhythms of the Brain*. Oxford university press; 2006.

4. Aru J, Aru J, Priesemann V, et al. Untangling cross-frequency coupling in neuroscience. *Current Opinion in Neurobiology*. 2015/04/01/ 2015;31:51-61. doi:https://doi.org/10.1016/j.conb.2014.08.002

5. Siems M, Pape A-A, Hipp JF, Siegel M. Measuring the cortical correlation structure of spontaneous oscillatory activity with EEG and MEG. *NeuroImage*. 2016/04/01/ 2016;129:345-355. doi:https://doi.org/10.1016/j.neuroimage.2016.01.055

6. Mormann F, Fell J, Axmacher N, et al. Phase/amplitude reset and theta–gamma interaction in the human medial temporal lobe during a continuous word recognition memory task. *Hippocampus*. 2005;15(7):890-900. doi:https://doi.org/10.1002/hipo.20117

7. Igarashi KM, Lu L, Colgin LL, Moser M-B, Moser EI. Coordination of entorhinal–hippocampal ensemble activity during associative learning. *Nature*. 2014/06/01 2014;510(7503):143-147. doi:10.1038/nature13162

8. Lisman John E, Jensen O. The Theta-Gamma Neural Code. *Neuron*. 2013/03/20/ 2013;77(6):1002-1016. doi:https://doi.org/10.1016/j.neuron.2013.03.007

9. Tort ABL, Komorowski RW, Manns JR, Kopell NJ, Eichenbaum H. Theta–gamma coupling increases during the learning of item–context associations. *Proceedings of the National Academy of Sciences*. 2009;106(49):20942. doi:10.1073/pnas.0911331106

10. Daume J, Kamiński J, Schjetnan AGP, et al. Control of working memory by phase-amplitude coupling of human hippocampal neurons. *Nature*. May 2024;629(8011):393-401. doi:10.1038/s41586-024-07309-z

11. Spyropoulos G, Bosman CA, Fries P. A theta rhythm in macaque visual cortex and its attentional modulation. *Proceedings of the National Academy of Sciences*. 2018;115(24):E5614-E5623. doi:doi:10.1073/pnas.1719433115

12. Kikuchi Y, Attaheri A, Wilson B, et al. Sequence learning modulates neural responses and oscillatory coupling in human and monkey auditory cortex. *PLOS Biology*. 2017;15(4):e2000219. doi:10.1371/journal.pbio.2000219

13. Nie JZ, Flint RD, Prakash P, et al. High-Gamma Activity Is Coupled to Low-Gamma Oscillations in Precentral Cortices and Modulates with Movement and Speech. *eneuro*. 2024;11(2):ENEURO.0163-23.2023. doi:10.1523/eneuro.0163-23.2023

14. Voytek B, Kayser AS, Badre D, et al. Oscillatory dynamics coordinating human frontal networks in support of goal maintenance. *Nature neuroscience*. 2015/09/01 2015;18(9):1318-1324. doi:10.1038/nn.4071

15. Salimpour Y, Anderson WS. Cross-Frequency Coupling Based Neuromodulation for Treating Neurological Disorders. *Front Neurosci*. 2019;13:125. doi:10.3389/fnins.2019.00125

16. van Wijk BCM, Beudel M, Jha A, et al. Subthalamic nucleus phase–amplitude coupling correlates with motor impairment in Parkinson's disease. *Clinical Neurophysiology*. 2016/04/01/ 2016;127(4):2010-2019. doi:https://doi.org/10.1016/j.clinph.2016.01.015

17. Morelli N, Summers RLS. Association of subthalamic beta frequency sub-bands to symptom severity in patients with Parkinson's disease: A systematic review. *Parkinsonism Relat Disord*. May 2023;110:105364. doi:10.1016/j.parkreldis.2023.105364

18. Chen P-L, Chen Y-C, Tu P-H, et al. Subthalamic high-beta oscillation informs the outcome of deep brain stimulation in patients with Parkinson's disease. Original Research. *Frontiers in human neuroscience*. 2022-September-08 2022;Volume 16 - 2022doi:10.3389/fnhum.2022.958521

19. Bocci T, Ferrara R, Albizzati T, et al. Asymmetries of the subthalamic activity in Parkinson's disease: phase-amplitude coupling among local field potentials. *Brain communications*. 2024;6(3):fcae201. doi:10.1093/braincomms/fcae201

20. Gong R, Wegscheider M, Mühlberg C, et al. Spatiotemporal features of β-γ phase-amplitude coupling in Parkinson's disease derived from scalp EEG. *Brain : a journal of neurology*. Mar 3 2021;144(2):487-503. doi:10.1093/brain/awaa400

21. de Hemptinne C, Ryapolova-Webb ES, Air EL, et al. Exaggerated phase-amplitude coupling in the primary motor cortex in Parkinson disease. *Proceedings of the National Academy of Sciences of the United States of America*. Mar 19 2013;110(12):4780-5. doi:10.1073/pnas.1214546110

22. de Hemptinne C, Swann NC, Ostrem JL, et al. Therapeutic deep brain stimulation reduces cortical phase-amplitude coupling in Parkinson's disease. *Nature neuroscience*. May 2015;18(5):779-86. doi:10.1038/nn.3997

23. Swann NC, de Hemptinne C, Aron AR, Ostrem JL, Knight RT, Starr PA. Elevated synchrony in Parkinson disease detected with electroencephalography. *Annals of neurology*. Nov 2015;78(5):742-50. doi:10.1002/ana.24507

24. Miller AM, Miocinovic S, Swann NC, et al. Effect of levodopa on electroencephalographic biomarkers of the parkinsonian state. *J Neurophysiol*. Jul 1 2019;122(1):290-299. doi:10.1152/jn.00141.2019

25. Duchet B, Bogacz R. How to design optimal brain stimulation to modulate phase-amplitude coupling? *Journal of Neural Engineering*. 2024/07/10 2024;21(4):046006. doi:10.1088/1741-2552/ad5b1a

26. Melgari JM, Curcio G, Mastrolilli F, et al. Alpha and beta EEG power reflects L-dopa acute administration in parkinsonian patients. *Frontiers in aging neuroscience*. 2014;6:302. doi:10.3389/fnagi.2014.00302

27. Stoffers D, Bosboom JL, Deijen JB, Wolters EC, Berendse HW, Stam CJ. Slowing of oscillatory brain activity is a stable characteristic of Parkinson's disease without dementia. *Brain : a journal of neurology*. Jul 2007;130(Pt 7):1847-60. doi:10.1093/brain/awm034

28. Postuma RB, Berg D, Adler CH, et al. The new definition and diagnostic criteria of Parkinson's disease. *The Lancet Neurology*. May 2016;15(6):546-8. doi:10.1016/s1474-4422(16)00116-2

29. Oostenveld R, Fries P, Maris E, Schoffelen JM. FieldTrip: Open source software for advanced analysis of MEG, EEG, and invasive electrophysiological data. *Computational intelligence and neuroscience*. 2011;2011:156869. doi:10.1155/2011/156869

30. Hülsemann MJ, Naumann E, Rasch B. Quantification of Phase-Amplitude Coupling in Neuronal Oscillations: Comparison of Phase-Locking Value, Mean Vector Length, Modulation Index, and Generalized-Linear-Modeling-Cross-Frequency-Coupling. Original Research. *Frontiers in Neuroscience*. 2019-June-07 2019;13doi:10.3389/fnins.2019.00573

31. Seymour RA, Rippon G, Kessler K. The Detection of Phase Amplitude Coupling during Sensory Processing. Original Research. *Frontiers in Neuroscience*. 2017-September-01 2017;11doi:10.3389/fnins.2017.00487

32. Glasser MF, Coalson TS, Robinson EC, et al. A multi-modal parcellation of human cerebral cortex. *Nature*. 2016/08/01 2016;536(7615):171-178. doi:10.1038/nature18933

33. Gramfort A, Papadopoulo T, Olivi E, Clerc M. OpenMEEG: opensource software for quasistatic bioelectromagnetics. *BioMedical Engineering OnLine*. 2010/09/06 2010;9(1):45. doi:10.1186/1475-925X-9-45

34. Veen BDV, Drongelen WV, Yuchtman M, Suzuki A. Localization of brain electrical activity via linearly constrained minimum variance spatial filtering. *IEEE Transactions on Biomedical Engineering*. 1997;44(9):867-880. doi:10.1109/10.623056

35. Loehrer PA, Nettersheim FS, Jung F, et al. Ageing changes effective connectivity of motor networks during bimanual finger coordination. *NeuroImage*. Dec 2016;143:325-342. doi:10.1016/j.neuroimage.2016.09.014

36. Loehrer PA, Nettersheim FS, Oehrn CR, et al. Increased prefrontal top-down control in older adults predicts motor performance and age-group association. *NeuroImage*. Jul 10 2021;240:118383. doi:10.1016/j.neuroimage.2021.118383

37. Hämäläinen MS, Ilmoniemi RJ. Interpreting magnetic fields of the brain: minimum norm estimates. *Medical & Biological Engineering & Computing*. 1994/01/01 1994;32(1):35-42. doi:10.1007/BF02512476

38. Tort ABL, Kramer MA, Thorn C, et al. Dynamic cross-frequency couplings of local field potential oscillations in rat striatum and hippocampus during performance of a T-maze task. *Proceedings of the National Academy of Sciences*. 2008;105(51):20517-20522. doi:doi:10.1073/pnas.0810524105

39. Kramer MA, Tort ABL, Kopell NJ. Sharp edge artifacts and spurious coupling in EEG frequency comodulation measures. *Journal of neuroscience methods*. 2008/05/30/ 2008;170(2):352-357. doi:https://doi.org/10.1016/j.jneumeth.2008.01.020

40. Jensen O, Spaak E, Park H. Discriminating Valid from Spurious Indices of Phase-Amplitude Coupling. *eneuro*. 2016;3(6):ENEURO.0334-16.2016. doi:10.1523/eneuro.0334-16.2016

41. Cole SR, van der Meij R, Peterson EJ, de Hemptinne C, Starr PA, Voytek B. Nonsinusoidal Beta Oscillations Reflect Cortical Pathophysiology in Parkinson's Disease. *The Journal of Neuroscience*. 2017;37(18):4830-4840. doi:10.1523/jneurosci.2208-16.2017

42. Lozano-Soldevilla D, ter Huurne N, Oostenveld R. Neuronal Oscillations with Non-sinusoidal Morphology Produce Spurious Phase-to-Amplitude Coupling and Directionality. Original Research. *Frontiers in Computational Neuroscience*. 2016-August-22 2016;10doi:10.3389/fncom.2016.00087

43. Chikermane M, Weerdmeester L, Rajamani N, et al. Cortical beta oscillations map to shared brain networks modulated by dopamine. eLife Sciences Publications, Ltd; 2024.

44. Benjamini Y, Hochberg Y. Controlling the false discovery rate: a practical and powerful approach to multiple testing. *Journal of the Royal statistical society: series B (Methodological)*. 1995;57(1):289-300.

45. Contarino MF, Bour LJ, Bot M, et al. Tremor-specific neuronal oscillation pattern in dorsal subthalamic nucleus of parkinsonian patients. *Brain stimulation*. Jul 2012;5(3):305-314. doi:10.1016/j.brs.2011.03.011

46. Asch N, Herschman Y, Maoz R, et al. Independently together: subthalamic theta and beta opposite roles in predicting Parkinson's tremor. *Brain communications*. 2020;2(2):fcaa074. doi:10.1093/braincomms/fcaa074

47. Karekal A, Miocinovic S, Swann NC. Novel approaches for quantifying beta synchrony in Parkinson's disease. *Experimental Brain Research*. 2022/04/01 2022;240(4):991-1004. doi:10.1007/s00221-022-06308-8

48. Binns TS, Köhler RM, Vanhoecke J, et al. Shared pathway-specific network mechanisms of dopamine and deep brain stimulation for the treatment of Parkinson's disease. *bioRxiv*. 2024:2024.04.14.586969. doi:10.1101/2024.04.14.586969

49. Oswal A, Beudel M, Zrinzo L, et al. Deep brain stimulation modulates synchrony within spatially and spectrally distinct resting state networks in Parkinson's disease. *Brain : a journal of neurology*. May 2016;139(Pt 5):1482-96. doi:10.1093/brain/aww048

50. Oswal A, Cao C, Yeh C-H, et al. Neural signatures of hyperdirect pathway activity in Parkinson's disease. *Nature Communications*. 2021/08/31 2021;12(1):5185. doi:10.1038/s41467-021-25366-0

51. Hollunder B, Ostrem JL, Sahin IA, et al. Mapping dysfunctional circuits in the frontal cortex using deep brain stimulation. *Nature neuroscience*. 2024/03/01 2024;27(3):573-586. doi:10.1038/s41593-024-01570-1

52. Canolty RT, Knight RT. The functional role of cross-frequency coupling. *Trends in cognitive sciences*. 2010/11/01/ 2010;14(11):506-515. doi:https://doi.org/10.1016/j.tics.2010.09.001

53. Loehrer PA, Weber I, Oehrn CR, et al. Microstructural alterations predict impaired bimanual control in Parkinson's disease. *Brain communications*. 2022;4(3):fcac137. doi:10.1093/braincomms/fcac137

54. Nettersheim FS, Loehrer PA, Weber I, et al. Dopamine substitution alters effective connectivity of cortical prefrontal, premotor, and motor regions during complex bimanual finger movements in Parkinson's disease. *NeuroImage*. Apr 15 2019;190:118-132. doi:10.1016/j.neuroimage.2018.04.030

55. Litvak V, Jha A, Eusebio A, et al. Resting oscillatory cortico-subthalamic connectivity in patients with Parkinson's disease. *Brain : a journal of neurology*. Feb 2011;134(Pt 2):359-74. doi:10.1093/brain/awq332

56. Cagnan H, Denison T, McIntyre C, Brown P. Emerging technologies for improved deep brain stimulation. *Nature Biotechnology*. 2019/09/01 2019;37(9):1024-1033. doi:10.1038/s41587-019-0244-6

57. Sharma R, Thirugnanasambandam N. Theta-Gamma Decoupling - A neurophysiological marker of impaired reward processing in Parkinson's disease. *Brain research*. Mar 1 2025;1850:149406. doi:10.1016/j.brainres.2024.149406

58. Spooner RK, Wilson TW. Cortical theta-gamma coupling governs the adaptive control of motor commands. *Brain communications*. 2022;4(6):fcac249. doi:10.1093/braincomms/fcac249

59. Bingham CS, Petersen MV, Parent M, McIntyre CC. Evolving characterization of the human hyperdirect pathway. *Brain structure & function*. Mar 2023;228(2):353-365. doi:10.1007/s00429-023-02610-5

60. Fischl B. FreeSurfer. *NeuroImage*. Aug 15 2012;62(2):774-81. doi:10.1016/j.neuroimage.2012.01.021

61. Tadel F, Baillet S, Mosher JC, Pantazis D, Leahy RM. Brainstorm: A User-Friendly Application for MEG/EEG Analysis. *Computational intelligence and neuroscience*. 2011/04/13 2011;2011:879716. doi:10.1155/2011/879716

Figure legends

Figure 1 Schematic overview of data collection and analysis. (A, left) EEG data were recorded using a high-density EEG with active electrodes. **(A, middle)** Individual structural MRI data were acquired. During MRI processing, the individual cortical surface was registered to the HCP-atlas to define regions of interest. **(A, right)** Artefact-free EEG and MRI data were co-registered by aligning the individual digitised electrode positions with the surface data to construct a realistic head model. **(B)** A linearly constrained minimum variance beamformer was used to extract source time series from a given ROI, and phase-amplitude coupling was examined using the Kullback-Leibler-based modulation index. Employing nonparametric permutation testing, we converted the ensuing modulation index-values to a z-score by comparing them to a surrogate distribution. An example of comparing PAC in M1 (green) between PD OFF and HC was shown here. **(C)** PAC values were derived for each subject by averaging the comodulograms of a given ROI and group statistics **(D)** were performed using a repeated measures and a mixed-design ANOVA. **(E)** The relationship between β-γ PAC and clinical features as well as treatment responses were examined using Spearman correlations. EEG = electroencephalography; HC = healthy controls; HCP =

human connectome project; OFF = Parkinson's disease patients in the OFF-medication state; PD ON = Parkinson's disease patients in the ON-medication state; PAC = phase-amplitude coupling; ROI = region of interest; ANOVA = analysis of variance.

Figure 2 Comparison of comodulograms between Patients with PD OFF medication and healthy controls. Group comodulograms displaying the modulation index (MI) across subjects for each group within the four regions of interest. The comodulograms represent z-scored MI (zPAC), obtained through nonparametric permutation testing where the observed MI-values were compared to a surrogate distribution of shuffled MI-values. Values > 0 indicate coupling stronger than null but are not necessarily significant, with relevance determined at the empirical 5% false positive threshold (which corresponds to a z-value of ~1.64). Brain regions with significant group differences, as assessed by post-hoc testing, are marked by an asterisk. For boxplots, zPAC values were averaged across hemispheres. The boxes represent the interquartile range (IQR), with the horizontal line indicating the median. Whiskers extend to 1.5 times the IQR or the most extreme data points within this range, while outliers are shown as individual points. DLPFC = dorsolateral prefrontal cortex; HC = healthy controls; lPM = lateral premotor cortex; M1 = primary motor cortex; OFF = Patients with Parkinson's disease in the OFF-medication state; PD ON = Patients with Parkinson's disease in the ON-medication state; SMA = supplementary motor area.

Figure 3 Comparison of comodulograms between Patients with PD OFF medication and Patients with PD ON medication. Group comodulograms displaying the modulation index (MI) across subjects for each group within the four regions of interest. The comodulograms represent z-scored MIs (zPAC), obtained through nonparametric permutation testing where the observed MI-values were compared to a surrogate distribution of shuffled MI-values. Values > 0 indicate coupling stronger than null but are not necessarily significant, with relevance determined at the empirical 5% false positive threshold (which corresponds to a z-value of ~1.64). Brain regions with significant group differences, as assessed by post-hoc testing, are marked by an asterisk. Please note that there was a trend towards significance for DLPFC (p = .052; marked by †). For boxplots, zPAC values were averaged across hemispheres. The boxes represent the interquartile range (IQR), with the horizontal line indicating the median. Whiskers extend to 1.5 times the IQR

or the most extreme data points within this range, while outliers are shown as individual points. DLPFC = dorsolateral prefrontal cortex; HC = healthy controls; lPM = lateral premotor cortex; M1 = primary motor cortex; OFF = Patients with Parkinson's disease in the OFF-medication state; PD ON = Patients with Parkinson's disease in the ON-medication state; SMA = supplementary motor area.

Figure 4 Correlation of high β-γ PAC changes in the SMA with UPDRS-III improvement. Relationship between the percentage change in high β-γ PAC within the SMA of the primarily affected side and the percentage change in UPDRS-III total scores and the bradykinesia-rigidity subscore. A greater reduction of high β-γ PAC in SMA was associated with a greater reduction in UPDRS-III total scores and bradykinesia-rigidity subscores. The solid black line represents the best-fit line while dashed lines represent 95% confidence intervals. P-values are corrected for multiple comparisons using the Benjamini-Hochberg method. PAC = phase-amplitude coupling; OFF = Patients with Parkinson's disease in the OFF-medication state; PD ON = Patients with Parkinson's disease in the ON-medication state; SMA = supplementary motor area; UPDRS = Unified Parkinson's Disease Rating Scale.

Figure 5 Source distribution of Mean PAC across Groups. z-transformed PAC values were extracted for high β-γ PAC, α-γ PAC, and θ-γ PAC averaged across patients (PD OFF and ON medication separately) and hemisphere. Subsequently, mean difference was calculated for each region by subtracting the mean ON value from the mean OFF value (OFF - ON). The complementary contrast (ON - OFF), shown alongside OFF - ON to emphasize directionality of effects, is provided in **Supplementary Figure 7**. Because raw MI is non-negative by definition, negative values can only occur here because we display z-transformed MI (zPAC, relative to a surrogate distribution) and then compute condition differences; thus, negative OFF-ON-values indicate higher zPAC in ON than OFF (and positive values indicate higher zPAC in OFF than ON), rather than "negative PAC". Data was then projected onto the parcellations of an example subject to visualise source distributions of PAC across different frequency bands. Visualisation clearly demonstrates the influence dopamine exerts on the cortical level and highlights that these effects are frequency specific within the investigated ROI (DLPFC, lPM, M1, SMA), with pronounced differences observed particularly in the high β-γ PAC range. Please note that the comparatively large zPAC values of high β-γ PAC mask the spatial distributions of α-γ and θ-

γ PAC. Corresponding maps with individually scaled colorbars are provided in **Supplementary Figure 6** to facilitate visualisation of these frequency bands. PAC = phase-amplitude coupling; OFF = Patients with PD in the OFF-medication state; PD ON = Patients with PD in the ON-medication state.

Table 1 Sociodemographic information of patients, severity of parkinsonism and standard medication

Patient ID	Age, years	Gender	UPDRS-III OFF	UPDRS-III ON	Disease duration, years	LEDD, mg
1	59	M	27	14	2	250
2	76	F	34	27	3	401
3	60	F	23	11	4	475
4	74	M	43	29	13	610
5	65	M	18	16	8	420
6	67	M	21	14	3	551
7	76	M	29	19	8	1200
8	48	M	36	26	7	940
9	65	M	34	16	10	300
10	80	M	18	12	3	310
11	68	M	32	15	11	500
12	76	M	42	23	6	475
13	64	M	19	16	1	40
14	69	M	18	7	4	322
15	76	M	16	17	9	800
Mean (SD)	68.2 (8.2)	–	27.3 (8.8)	17.5 (6.0)	6.1 (3.5)	506 (281)

F = female; LEDD = Levodopa equivalent daily dose; M = male; UPDRS-III = Unified Parkinson's Disease Rating Scale part III.

Table 2 Post-hoc comparison of high β-γ PAC between groups

HC versus PD-OFF			PD-ON versus PD-OFF		
Connection	***P***	**Effect size**	**Connection**	***P***	**Effect size**
M1-IPM	0.042	0.66	**M1-DLPFC**	0.008	0.554
IPM-M1	0.042	0.62	**DLPFC-M1**	0.018	0.675
DLPFC-M1	0.042	0.58	**M1-IPM**	0.018	0.555
DLPFC-IPM	0.042	0.553	**SMA-DLPFC**	0.018	0.545
M1-DLPFC	0.042	0.562	**DLPFC-SMA**	0.021	0.529
IPM-DLPFC	0.055	0.502	**IPM-M1**	0.025	0.602
			DLPFC-IPM	0.036	0.494
			IPM-DLPFC	0.052	0.402
			M1-SMA	0.056	0.356
			SMA-IPM	0.057	0.349

t-tests were employed to compare healthy controls (HC) and patients with PD OFF medication, while paired t-tests were used to compare between patients with PD ON and OFF medication. *P*-values were corrected for multiple comparisons using the Benjamini-Hochberg method. Bold font indicates significant *P*-values after adjustment for multiple comparisons.

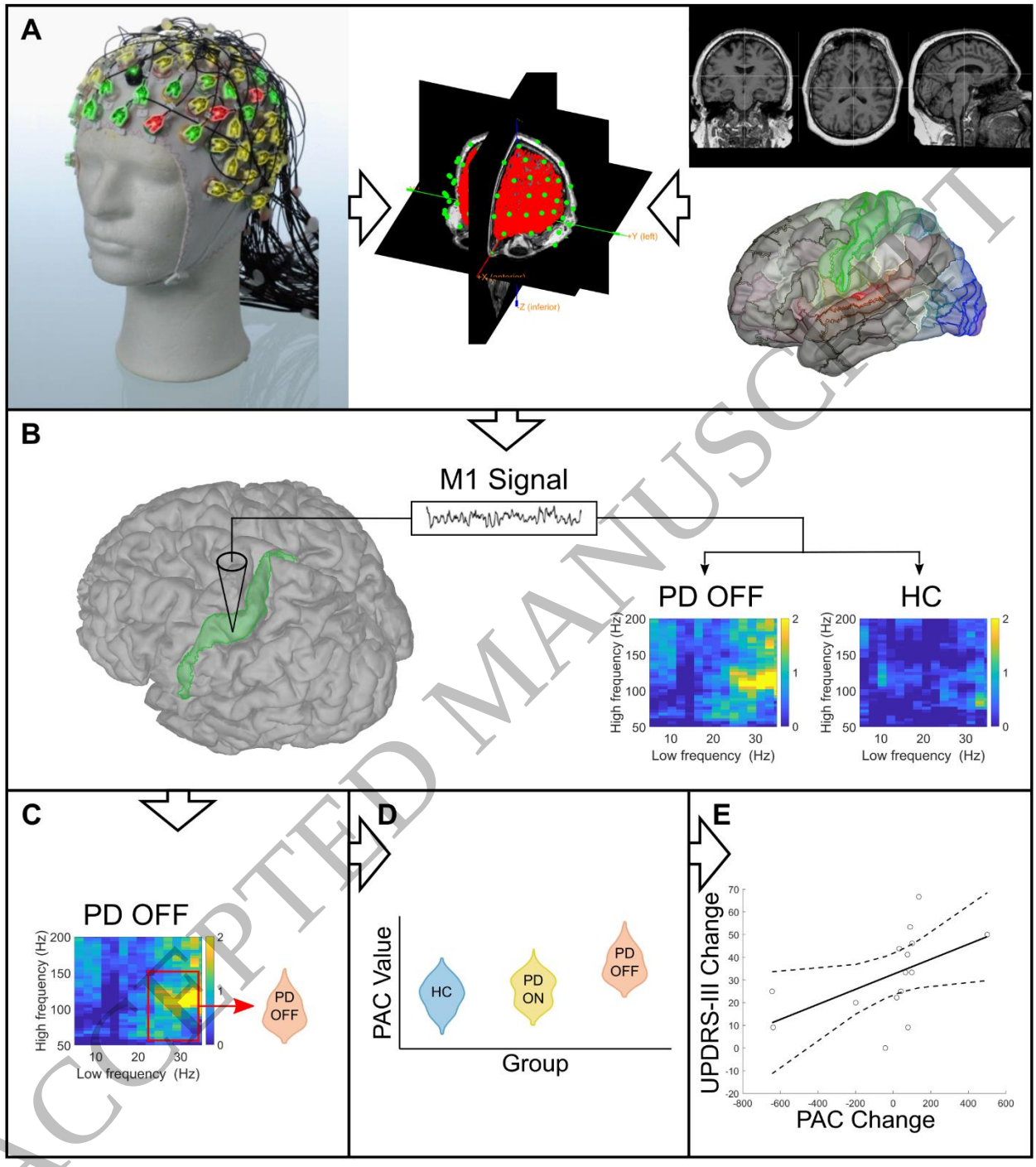

Figure 1
165x186 mm (x DPI)

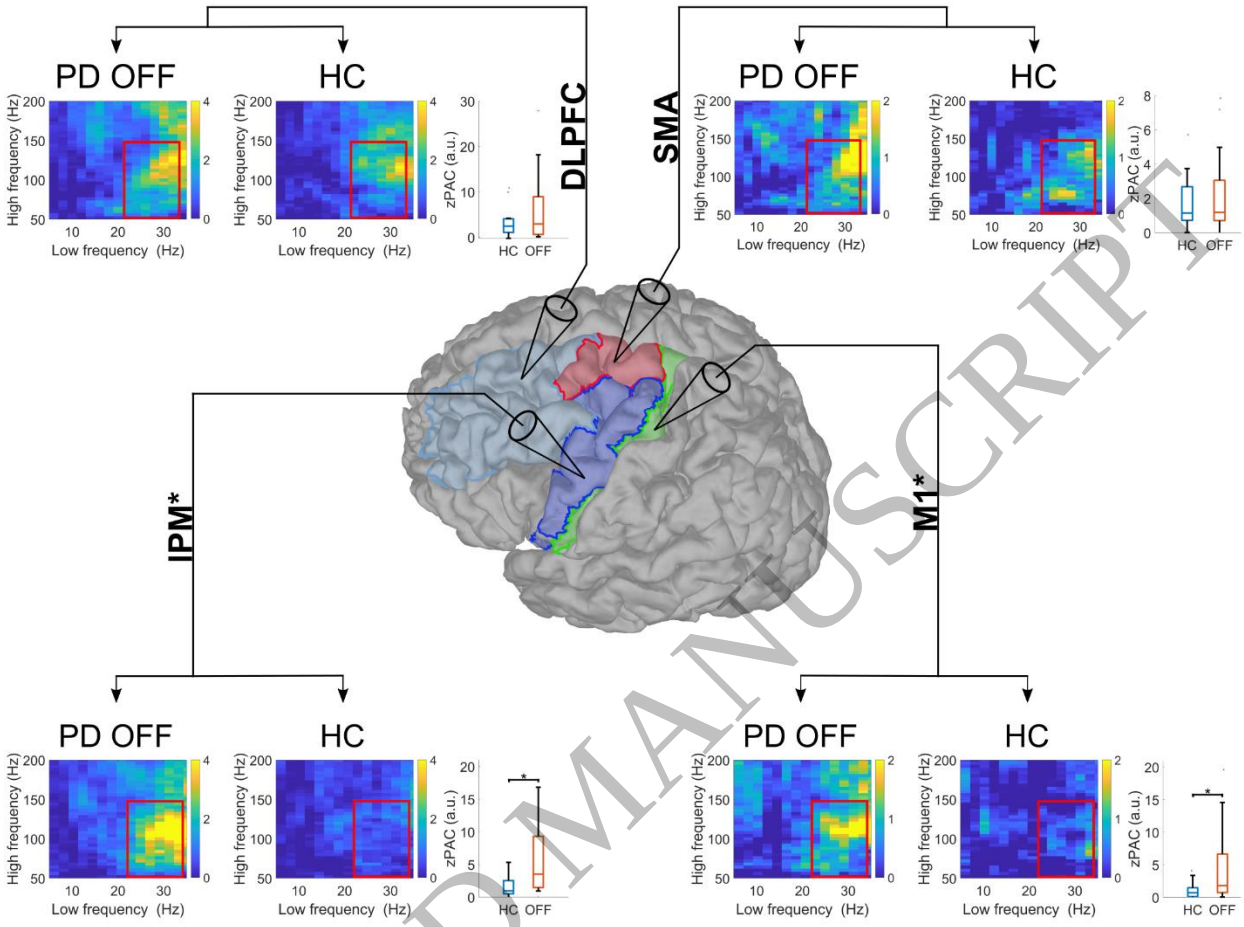

Figure 2
165x132 mm (x DPI)

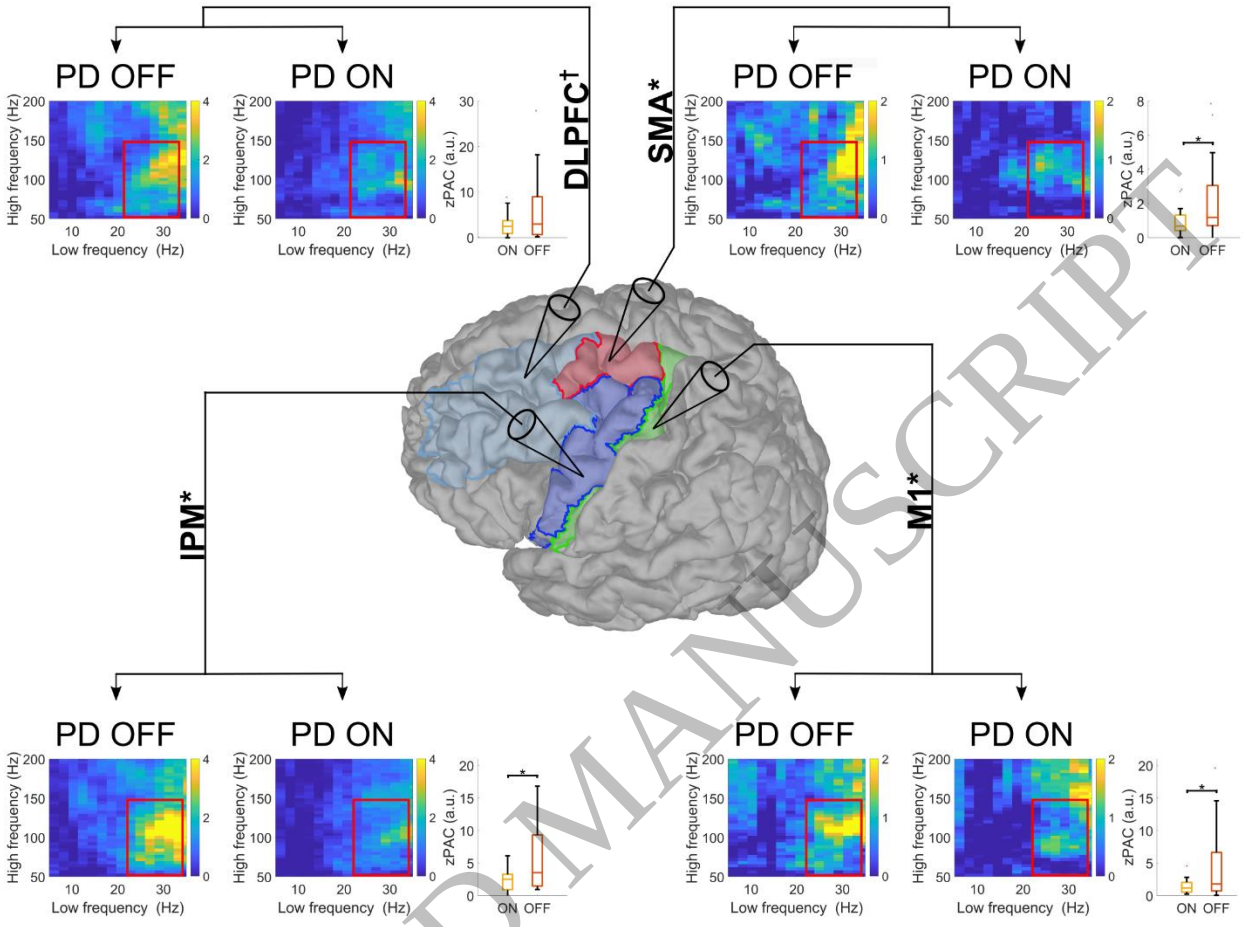

Figure 3
165x132 mm (x DPI)

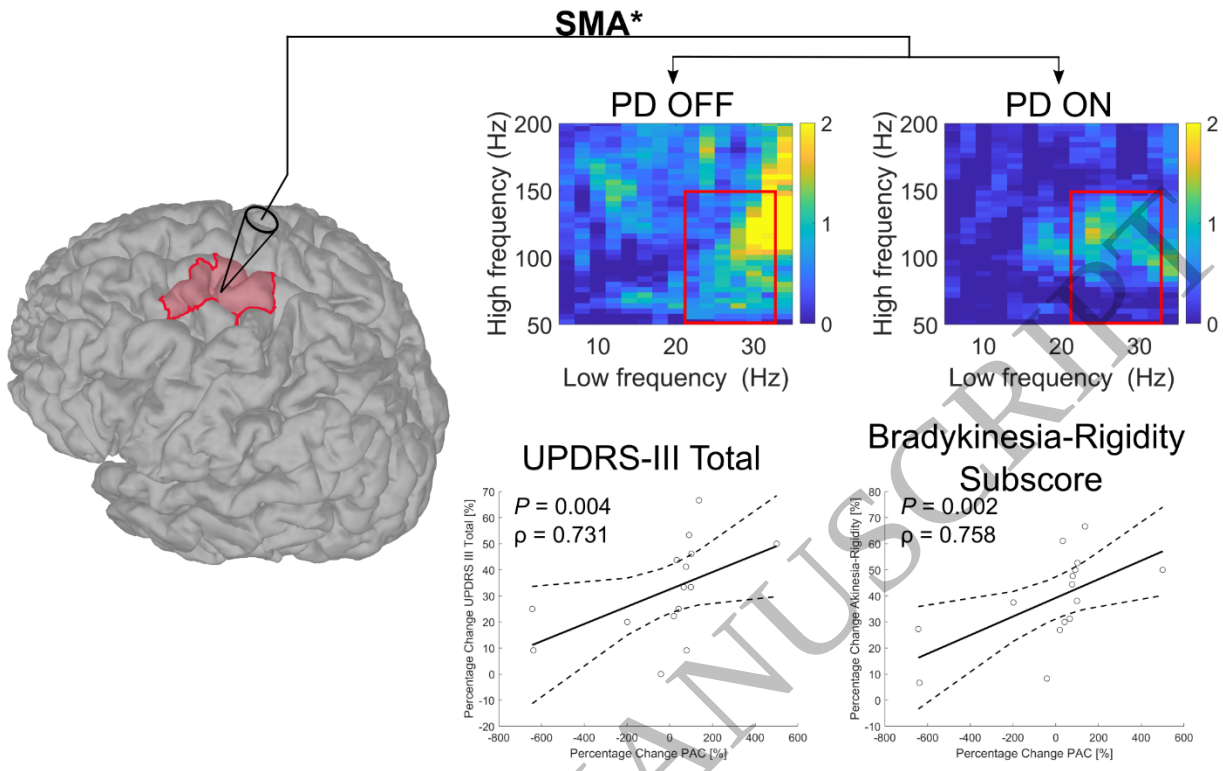

Figure 4
165x101 mm (x DPI)

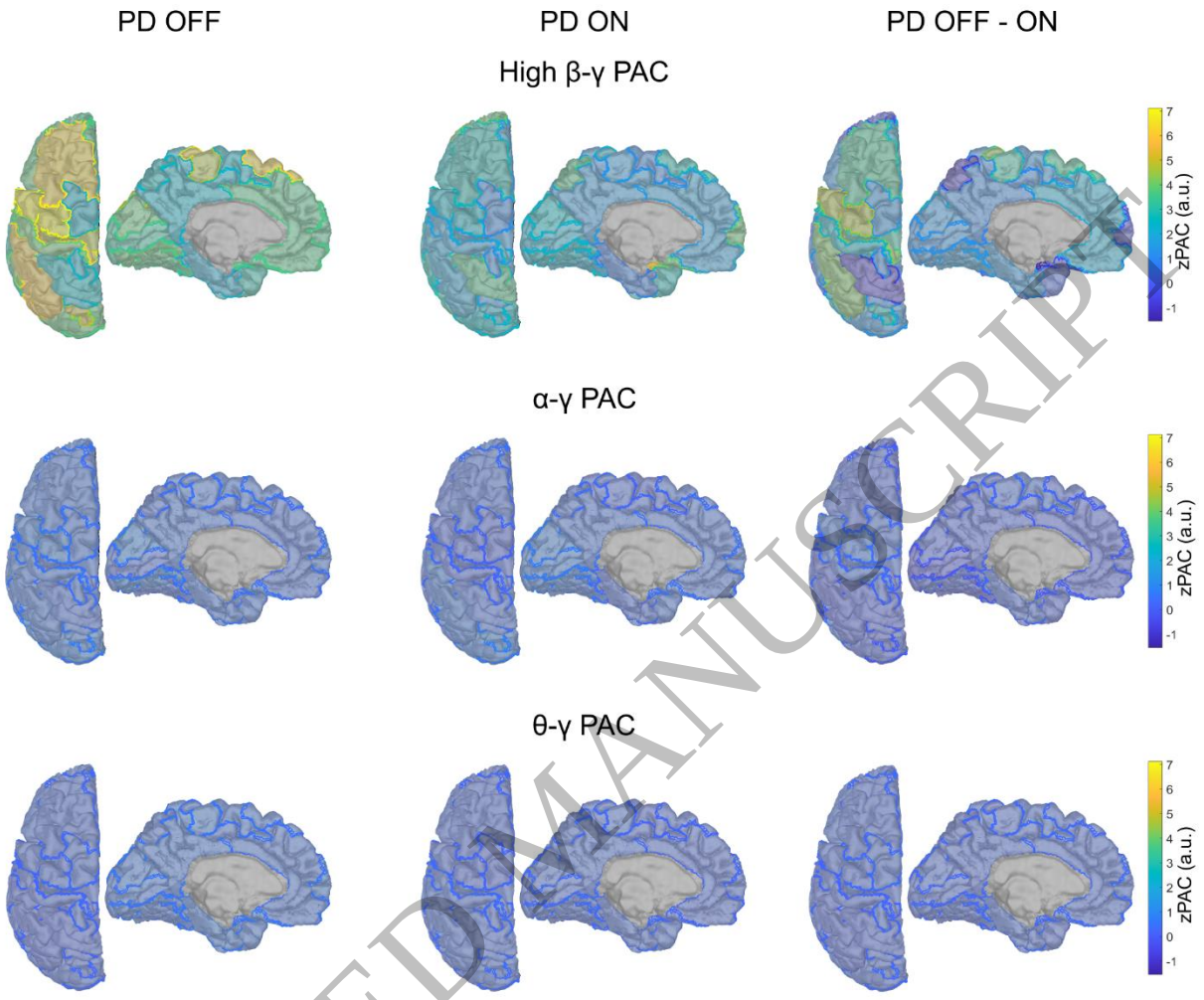

Figure 5
165x138 mm (x DPI)